Influence of Spontaneous Curvature and Microtubules on the Conformations of Lipid Vesicles

W. T. Góźdź*

Institute of Physical Chemistry Polish Academy of Sciences, Kasprzaka 44/52, 01-224 Warsaw, Poland

Received: May 23, 2005; In Final Form: August 1, 2005

The conformations of vesicles deformed by microtubules are studied within the framework of the curvature energy. The phenomenon in which the destruction of a microtubule is followed by the formation of peristaltic shapes on a protrusion created by the microtubule is investigated. The influence of the spontaneous curvature on the conformations of vesicles is examined, and the results are compared to existing experiments. The elastic properties of a vesicle deformed by the microtubule are studied.

1. Introduction

Microtubules are rigid, cylindrical aggregates of the protein tubuline. They are thin, long, and rigid objects which can be found in biological systems. When microtubules are encapsulated inside lipid vesicles,[1] they can grow due to the polymerization of the tubuline and deform vesicles when the size of a microtubule is larger than the distance between the walls of a vesicle.[1−4] Tubular membrane protrusions are created due to the deformation of a vesicle by microtubules. The length of the protrusions depends mainly on the length of the microtubule. A few types of deformations have been observed. When two ends of the rigid microtubule deform a vesicle, it may change its shape from a spherical one to a vesicle which resembles the greek letter ϕ or a dumbbell. It is also possible that only one end of the microtubule creates a protrusion. In such a case, a vesicle transforms into a new vesicle with the shape which resembles a cherry. Such transitions have been already investigated both experimentally and theoretically.[1−4] This study is motivated by the phenomenon observed in the experiment in which it was demonstrated that after the destruction of the microtubule which created a cylindrical protrusion, the shape of the cylindrical protrusion changed into a peristaltic one.[5] The peristaltic shapes may indicate that the curvature of the membrane is high enough to form such shapes.[6,7] The peristaltic shapes are present in many experimental situations. They can be formed from cylindrical membranes by means of many different physical mechanisms and different stimuli. It has been demonstrated experimentally that tubular polymersomes[8,9] undergo a shape transition, induced by lowering the temperature from a cylinder to a chain of connected beads.[10] The action of laser tweezers[11−13] or the presence of hydrophilic polymers with hydrophobic side groups[14,15] induce the transformations from cylinders to beads. The laser tweezers touching a surface of a membrane exert some tension on the membrane, which results in the formation of peristaltic shapes on the cylindrical membrane. This phenomenon is called pearling instability. Polymers attached to a membrane may induce the spontaneous curvature, which results in a change of the membrane shape.

In the former theoretical studies of vesicles deformed by microtubules,[2−4] it is assumed that the spontaneous curvature of the membrane is zero. The investigations have focused mainly on the shape deformation caused by the growing microtubule. It has not been attempted to examine the shape or the shape relaxation after a destruction of a microtubule. The experiment shown in ref 5 indicates the possibility that the spontaneous curvature of the membrane deformed by a microtubule may not be zero. It has been demonstrated that the destruction (after irradiation by UV) of the microtubule which formed cylindrical protrusion resulted in the change of its shape from a cylindrical to peristaltic one. Such peristaltic shapes are present when the curvature of a membrane is not zero.[6,7] One may speculate that the spontaneous curvature is induced when the membrane is deformed by the microtubule or when the membrane is irradiated. So far, it has not been examined how the spontaneous curvature would modify the behavior of vesicles containing microtubules. The purpose of this article is to perform model calculations to investigate the situation where microtubules deform a vesicle characterized by a high spontaneous curvature.

The ensemble which is chosen to mimic the experimental situation is the one with constant surface area S and volume V of a vesicle. It has been assumed that a bilayer membrane is hardly stretchable and the volume of the vesicle does not change. The presence of microtubules inside a vesicle is modeled by imposing the constraint which restricts the distance between the poles of the vesicles so that it cannot be smaller than the length of a microtubule, T. Such a physical situation may be modeled by the elastic energy[16−18] given by

$$\mathcal{F} = \frac{\kappa}{2}\int_S \mathrm{d}S(C_1 + C_2 - C_0)^2 \qquad (1)$$

where κ is the bending rigidity, C_1 and C_2 are the principal curvatures, and C_0 is the spontaneous curvature, and the integral (1) is taken over the surface of a closed vesicle. No topology changes are allowed; therefore, the integral over the Gaussian curvature contributes a constant value and is omitted in eq 1.

2. Parametrization

The nature of the problem imposes the rotational symmetry of a vesicle. Therefore, in this study only axisymmetric vesicles are considered. A vesicle shape can be well approximated in numerical calculations by closed surfaces which are rotationally symmetric. It is convenient to parametrize their shape with the angle between the rotation axis and the line tangent to the shape

* E-mail: wtg@ichf.edu.pl.

10.1021/jp052694+ CCC: $30.25
Published on Web 10/14/2005

profile, $\theta(s)$, as a function of the arc length, s. The radius $r(s)$ and the height $z(s)$ of the shape profile are calculated from $\theta(s)$ according to

$$r(s) = \int_0^s \mathrm{d}s' \cos(\theta(s')) \tag{2}$$

$$z(s) = \int_0^s \mathrm{d}s' \sin(\theta(s')) \tag{3}$$

To parametrize a closed shape, the following boundary conditions must be satisfied

$$\theta(0) = 0 \tag{4}$$

$$\theta(L_s) = \pi \tag{5}$$

$$r(L_s) = 0 \tag{6}$$

where L_s is the length of the shape profile. Eqs 4 and 5 guarantee that the profile is smooth at the ends, and eq 6 accounts for the fact that the vesicle is closed.

Functional 1 with the shape profile parametrized by $\theta(s)$ is given by

$$\mathscr{F} = \frac{\kappa}{2}(2\pi)\int_0^{L_s} \mathrm{d}s r(s)\left(\frac{\mathrm{d}\theta(s)}{\mathrm{d}s} + \frac{\sin(\theta(s))}{r(s)} - C_0\right)^2 \tag{7}$$

The experimental conditions we would like to mimic are such that the surface area S and volume V are constant. It is assumed that no osmotic pressure is present in the system and that the membrane does not stretch significantly. It is assumed that microtubules are rigid and located inside a vesicle along the rotation axis. We consider equilibrium states in which microtubules have a given length and do not shrink or grow and the shape of the vesicle has reached its equilibrium state. It is assumed that the growth of a microtubule is slower than the shape relaxation of a vesicle. When a microtubule grows, it acts on the membrane in such a way that the distance between the poles of a vesicle $z(L_s)$, which are located at the intersection of the rotation axis and the membrane surface, is always bigger than the microtubule length T. It can be written as the following constraint

$$z(L_s) \geq T \tag{8}$$

The minima of functional 7 are interpreted as equilibrium configurations observed in experiments. Functional 7 is minimized numerically. The function describing the shape profile $\theta(s)$ is approximated by the Fourier series

$$\theta(s) = \theta_0 \frac{s}{L_s} + \sum_{i=1}^{N} a_i \sin\left(\frac{\pi}{L_s} is\right) \tag{9}$$

where N is the number of the Fourier modes, and a_i values are the Fourier amplitudes. θ_0 is the angle at the south pole of the vesicle, $\theta_0 = \pi$. When the function $\theta(s)$, in the form of the Fourier series given by eq 9, is plugged in to eqs 2, 3, and 7, the functional minimization can be replaced by the minimization of the function of many variables. Functional 7 becomes the function of many variables which are the amplitudes a_i and the length of the shape profile L_s. The minimization is performed under the constraints of constant surface area S and volume V and the length of the tubule T where

$$S = 2\pi \int_0^{L_s} \mathrm{d}s r(s) \tag{10}$$

$$V = \pi \int_0^{L_s} \mathrm{d}s r^2(s) \sin\theta(s) \tag{11}$$

The constraints in numerical calculations are implemented with the help of Lagrange multipliers. Simple shapes, resembling a sphere, are easily parametrized with a few coefficients, a_i, in the series. A large number of the amplitudes, on the order of 100, is required in order to accurately parametrize complex shapes. It has to be noted that the minimization of functional 1 for the complex shapes and with a few nonlinear constraints is not a trivial task. There are four nonlinear constraints which have to be taken into account during minimization, the constraint for surface area, volume, and length of the microtubule and the constraint for the closed contour of the shape profile, which is more difficult to implement when up and down symmetry of the profile is not employed. Here, the minimization is performed with a high accuracy which is computationally expensive for surfaces characterized by high spontaneous curvature. It is important to use a proper Fourier series which approximates the set of functions which describe the investigated vesicle shape in order to make the numerical calculations easier. It is required by the physics of the problem that $\theta(0)$ must be zero to make the profile smooth at the north pole of the vesicle. A proper series is one which by construction fulfills boundary conditions for the shape profile, i.e., $\theta(0) = 0$ and $\theta(L_s) = \pi$. For example, the cosine series is not a good choice since, for $s = 0$, $\theta(0) \neq 0$ by construction. The sine series almost perfectly fulfills the requirements for the set of functions for which we are looking.

The volume, V_0, and the radius, R_0, of the sphere having the same surface area S as the investigated vesicle, are chosen as units of volume and length, respectively.[19,20]

$$R_0 = \sqrt{S/4\pi} \tag{12}$$

$$V_0 = \frac{4}{3}\pi R_0^3 \tag{13}$$

The dimensionless, reduced volume v, the spontaneous curvature c_0, and the length of a microtubule t are defined as

$$v = V/V_0 \tag{14}$$

$$c_0 = C_0 R_0 \tag{15}$$

$$t = T/R_0 \tag{16}$$

Thus, there are three control parameters important for the process, t, v, and c_0, since the model is scale invariant. Since the number of controlled parameters is higher than in the usual studies of vesicles, they have to be carefully chosen.

3. Results

We examine the influence of the spontaneous curvature on the vesicle containing the microtubule (section 3.1) and the influence of the microtubules of a different length on the vesicle with high spontaneous curvature (section 3.2). It is done by minimizing functional 7 with appropriate constraints on the microtubule length T, volume V, and surface area S.

3.1. Varying the Spontaneous Curvature at Constant Length of a Microtubule. The vesicles with encapsulated microtubules have been studied experimentally[1−3] and theoretically.[4] The theoretical studies presented here are inspired by the experiment reported in ref 5, in which the microtubule that deformed a vesicle was destroyed and the shape of the protrusion changed from a cylindrical to peristaltic one. The calculations,

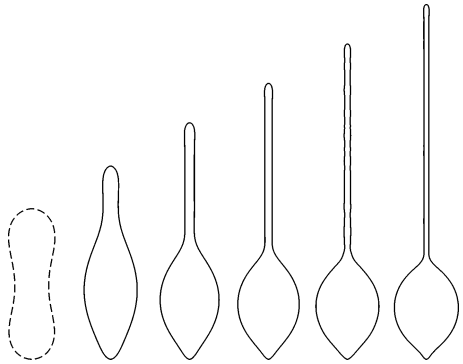

Figure 1. Shape profiles with different lengths of a microtubule for the reduced volume $v = 0.7$ and the spontaneous curvature $c_0 = 0$. The first profile, denoted by the dashed line, represents the configuration without a microtubule. The lengths of the microtubule are $t = 4.9$, $t = 6.0$, $t = 7.0$, $t = 8.0$, and $t = 9.0$ for the subsequent configurations from the left to the right. 160 amplitudes were used to parametrize the shape profile for minimization of functional 7.

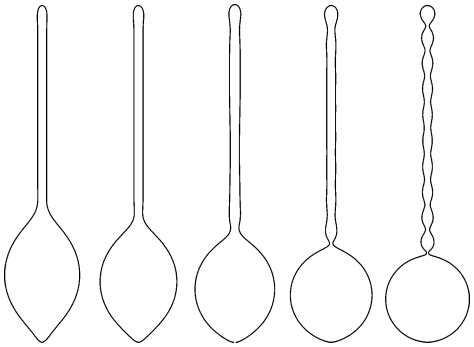

Figure 2. Influence of the spontaneous curvature on the shape of a vesicle containing a microtubule. The spontaneous curvatures for the presented shape profiles are $c_0 = 0$, $c_0 = 3$, $c_0 = 6$, $c_0 = 9$, and $c_0 = 12$, starting from the left side. The length of the microtubules is $t = 7.0$, and the reduced volume is $v = 0.7$. 320 amplitudes were used in the calculations.

presented in Figure 1, are performed for $c_0 = 0$ in order to check if it is possible to find the shape which resembles the shape of the vesicle containing the microtubule, observed in experiment.[5] The reduced volume, $v = 0.7$, is chosen to mimic roughly the shape of the vesicle published in ref 5. It has been shown in ref 4 and is confirmed here that for the reduced volume $v = 0.7$ and spontaneous curvature $c_0 = 0$, the protrusion develops only at one pole of the vesicle. Thus, the mirror symmetry for the empty vesicle (see the first profile in Figure 1) with respect to the symmetry plane located at the equator of the vesicle is spontaneously broken when a microtubule begins to deform the vesicle. The shape with protrusions on both poles of the vesicle are metastable.[4] The configurations of the vesicles with microtubules of different sizes are shown in Figure 1.

A similar problem has been considered in ref 21, where the vesicle of a large reduced volume, $v = 0.95$, has been deformed by attaching it to two glassy surfaces separated by some distance or deformed by the force acting on a magnetic bead attached to the vesicle. In the first case, the analysis presented here may also be applied with the constraint $z(L_s) = T$ which is different from the constraint used in the present study $z(L_s) \geq T$. Moreover, the parameter space examined in ref 21 was restricted to protrusions with cylindrical shapes. Here, we are mostly interested in protrusions with a beadlike structure.

The configurations with $c_0 = 0$ do not resemble the experimental picture from ref 5, both with and without the microtubule. That difference may result from the fact that inside the vesicle there is a bundle of microtubules and they are not infinitely stiff as modeled in the theoretical calculations. It is also possible that the spontaneous curvature is not zero. Such a possibility is hinted by the shape of the vesicle after destruction of the microtubules.

Figure 2 shows the configuration of vesicles with different spontaneous curvatures and the same microtubule length $t = 7.0$. When the length of a microtubule is kept constant and the spontaneous curvature is varied, one may observe a certain tendency in the change of the vesicle shape. It changes in such a way that initially the protrusion remains cylindrical and the vesicle becomes more spherical. The volume and the surface area of the protrusion and the spherical part of the vesicle are changed. When the spontaneous curvature is sufficiently high for a given length of the protrusion, the beads are formed on the protrusion, such as on the last profile in Figure 2. Thus, by analyzing the shapes of vesicles containing microtubules, one may gain some knowledge about the spontaneous curvature of the membrane.

It is interesting to know whether the vesicles with protrusions composed of many small beads (such as the vesicle with the spontaneous curvature $c_0 = 12$ in Figure 2) are formed only when the protrusion contains a microtubule. In the next section, such problem is carefully examined.

3.2. Varying the Length of a Microtubule at Constant Spontaneous Curvature. By analyzing the shape of the vesicle with the destroyed microtubule, presented in ref 5, one may expect, based on the previous studies,[20,22] that the spontaneous curvature of the vesicle is high. The phase diagram of axisymmetric vesicles with low spontaneous curvature has been already investigated,[19,20] but the phase diagram for large spontaneous curvature is still not thoroughly explored. Increasing the spontaneous curvature leads to shapes which look like a chain of small beads connected with a larger sphere according to the calculations performed here. If the reduced volume is set constant, then the size of the beads and the number of beads depend on the spontaneous curvature. The larger the spontaneous curvature, the larger the number of small beads present in the configurations with the lowest energy. The spontaneous curvature $c_0 = 12$ was chosen in the present study since for this value of c_0 and $v = 0.7$ the shape profile for the minimum of functional 7, which has the lowest energy, is the one with eight small beads attached to a large sphere. Hence, it resembles the shape of the vesicle observed in experiments reported in ref 5. However, the conclusions presented here are also valid for the vesicles characterized by similar values of the spontaneous curvature and the reduced volume.

The mechanism arising such a large spontaneous curvature, in the vesicle described in ref 5, is unclear. There are two hypotheses. It is possible that a growing microtubule may stretch the membrane and in such a new geometry some lipids from the inner layer of the bilayer may flip-flop to the outer layer. It is also possible that during irradiation by UV, the high spontaneous curvature arises in the bilayer.[23] The molecular mechanism for arising the spontaneous curvature is not known in this case. One may speculate that membrane constituents undergo conformational changes. However, to determine the actual mechanism, additional experiments should be performed.

When the spontaneous curvature is sufficiently high, there exist many minima of functional 7. Figure 3 shows the shape profiles for the minima of functional 7 at the reduced volume $v = 0.7$, the spontaneous curvature $c_0 = 12$, and without the

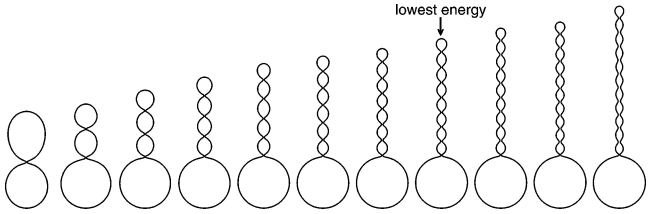

Figure 3. Shape profiles corresponding to the local minima of functional 7 for the reduced volume $v = 0.7$, the spontaneous curvature $c_0 = 12$, and without the constraint for the length. 320 amplitudes were used to parametrize the shape profiles. The solution with the lowest energy is the one with 8 small beads.

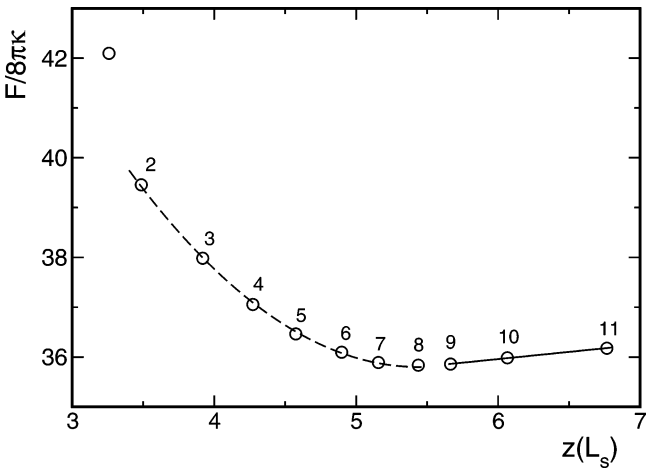

Figure 4. Local minima of the curvature energy F as a function of the distance between the poles of the vesicle $z(L_s)$ (without the constraint (8)). The open circles represent the minima of functional 7 corresponding to the profiles shown in Figure 3. The dashed line is the fit to the points with 2, 3, 4, 5, 6, 7, and 8 small beads of the parabolic curve $F = B/2(z - z_8)^2 + F_0$, where $B = 0.47(8\pi\kappa)$ and $z_8 = z(L_s)$ for the profile with 8 small beads. The solid line is the fit to the points with 9, 10, and 11 small beads of the straight line. The numbers above the symbols indicate the number of small beads.

constraints for the length. All the configurations except the first one look similar, since they are composed of a large sphere connected with a chain of beads. The size of small beads and the distance between the poles of the vesicle is different for each minimum. Of course, for a given spontaneous curvature, the size of the beads cannot be arbitrarily small. The existence of so many metastable states is possible due to the presence of the large sphere which acts as a volume and surface reservoir for the long protrusion. The global minimum is the configuration with eight small beads, but there exist local minima with a larger number of beads and thus with a bigger distance between the poles of the vesicle, as shown in Figure 4. Similar profiles have been considered in refs 20 and 22 but with a lower number of small beads.

It is interesting to note that on the energy−distance plot (Figure 4), the points which represent configurations with a smaller number of beads rather than the configuration which is the global minimum are very well approximated with the parabolic curve shown by the dashed line. Thus, one may speculate that in some hypothetical process of compressing the stable configuration (the one with the lowest energy), the vesicle behaves asymptotically according to Hook's law, that is, the force which causes the deformation is proportional to the change of the distance between the poles. The transitions between the minima with a different number of beads will proceed through a series of metastable states. The energy of those metastables states will be in general a complex function of the pole-to-pole

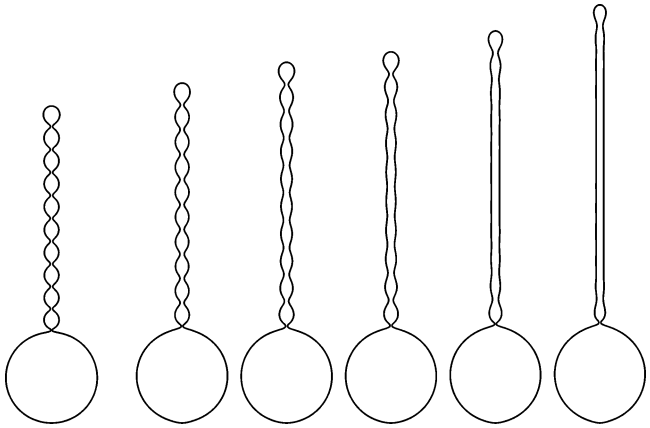

Figure 5. Deformation of the vesicle, composed of 10 small beads, by a microtubule of different lengths. The spontaneous curvature and the reduced volume are $c_0 = 12$ and $v = 0.7$, respectively. The first profile represents the configuration with 10 beads without the microtubule. In the subsequent profiles, the lengths of the enclosed microtubule are $t = 6.5$, $t = 6.9$, $t = 7.1$, $t = 7.5$, and $t = 8.0$.

distance, which differs from the energy curve resulting from the extrapolation of the minima with a different number of beads, denoted by the dashed line in Figure 4.

One may expect that Hook's Law is also obeyed during the stretching of the vesicle, for example, by the microtubules encapsulated inside that vesicle. Such a hypothesis is carefully checked in the remaining part of this section. When we consider the situation in which the length of the microtubule T is larger than the distance $z(L_s)$ between the poles of the vesicle with eight small beads (without the microtubule inside), it may be possible that with the microtubule inside a vesicle, a configuration with a number of beads larger than eight becomes the global minimum. Thus, the increase of the length of the microtubule may induce a shape transition. Indeed, it is possible to find more than one local minimum for the same values of the reduced volume v, the spontaneous curvature c_0, and the length of the microtubule t. Different minima correspond to a different number of beads. When the microtubule becomes sufficiently long, the protrusion which is formed of beads begins to change in such a way that the middle part of it becomes cylindrical and the beads are present only at the ends of the protrusion, as shown in Figure 5. It is interesting to note that the shape transformations of tubular polymersomes, observed experimentally in ref 10 and described theoretically in ref 24, look surprisingly similar to the transformations described above, despite a different geometry and a different physical mechanism of the transformation. The reduced volume of the vesicles differs substantially; the vesicles in ref 10 have up−down symmetry while that in ref 5 does not. The vesicle in ref 5 is stretched by a microtubule while those in ref 10 are tensionless. In ref 10, the spontaneous curvature is changed by the temperature, while in ref 5 the spontaneous curvature is constant and the vesicle is deformed by a microtubule. If it were possible to control the growth of the microtubule inside the vesicle with high spontaneous curvature, then it should be possible to change the structure of the protrusion from beads to cylinder and vice versa. Alternatively, it can be also done by pulling the protrusion. A further increase in the length of the microtubule leads to the cylindrical shape of the protrusion, with no beads at its ends. The radius of the cylindrical protrusion decreases with increasing length of the protrusion.

When the vesicle is stretched, the energy grows linearly with the distance when the protrusion has a structure of connected beads. The points representing energy for configurations with

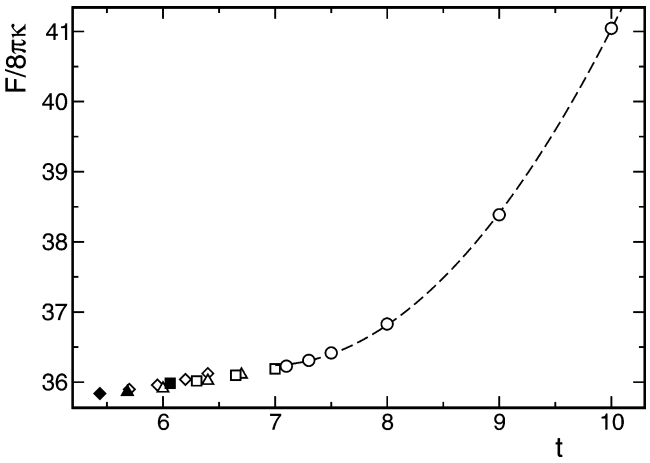

Figure 6. Curvature energy F, as a function of the microtubules length t, for the vesicle with the high spontaneous curvature $c_0 = 12$ and the reduced volume $v = 0.7$. The solid diamond, triangle, and square represent the minima of functional 7 without constraint 8 and with the corresponding profiles shown in Figure 3, for 8, 9, and 10 small beads, respectively. The open diamonds, triangles, and squares represent the minima of functional 7 for configurations with 8, 9, and 10 small beads, respectively, with the microtubule inside the vesicle. The open circles represent the minima of functional 7 for the configuration with the cylindrical protrusion created by the microtubule. The dashed line is a fit of the parabolic curve to the points denoted by the open circles. 320 amplitudes were used to parametrize the shape profile.

8, 9, and 10 beads (denoted by diamonds, triangles, and squares) in Figure 6 lie approximately on the straight lines. When the protrusion is sufficiently stretched ($T > z_{11}$, where z_{11} is the pole-to-pole distance $z(L_s)$ of the configuration with 11 small beads without the microtubule inside), the beads disappear and the protrusion is cylindrical. A few minima with cylindrical protrusion calculated for a few lengths of the microtubule are very well approximated by the parabolic curve denoted by the dashed line in Figure 6. It is possible to calculate additional minima for a different length of the microtubule, which will lie on the parabolic curve. It has not been done just to reduce the time for computations. Thus, it is plausible that in real systems the process of stretching the vesicle by the microtubule will proceed according to the presented scenario. The energy of stretching (or pulling) of the cylindrical protrusion is proportional to the squared distance, and the vesicle behaves according to Hook's law.

During the stretching process of the vesicle with 8 small beads, one should observe a series of phase transitions, two discontinuous from 8 to 9 and from 9 to 10 beads and finally the continuous transition from 10 beads to cylindrical protrusion. The continuous transition is pictured in Figure 5. It has to be noted that the vesicle with 11 beads has higher curvature energy than the stretched vesicle with 10 beads. The differences in curvature energy between the local minima for configurations with 8, 9, or 10 beads and the encapsulated microtubule are very small at most on the order $0.06(8\pi\kappa)$. Therefore, one may expect that the shape transformations between them can be easily induced by small stimuli. We hope that the model calculations presented here will help to understand transformations of vesicles observed in experiments and to design new experiments. For example, it would be interesting to investigate the influence of UV irradiation on the lipid membrane by examining the shape of the protrusion which can be created spontaneously or by a microtubule or by mechanical pulling of the membrane.

4. Summary and Conclusions

The influence of microtubules and the spontaneous curvature on vesicles with the reduced volume $v = 0.7$ has been investigated. The existence of metastable states for vesicles with high spontaneous curvature has been examined in detail for the spontaneous curvature $c_0 = 12$. In the system with many metastable states, an extra constraint, due to the presence of microtubule, may stabilize some and destabilize other conformations. The elastic properties of vesicles deformed by microtubules have been studied. It has been shown that the vesicles which have a long protrusion composed of beads do not obey Hook's law when they are stretched. When the protrusion is cylindrical, the vesicle is stretched according to Hook's law. We hope that the model calculations which are described here may serve as a guide in understanding similar phenomena.

Acknowledgment. The author acknowledges support from the Polish State Committee for Scientific Research 3 T09A 069 27 in 2004−2006.

References and Notes

(1) Hotani, H.; Miyamoto, H. *Adv. Biophys.* **1990**, *26*, 135.
(2) Kuchnir Fygenson, D.; Marko, J. F.; Libchaber, A. *Phys. Rev. Lett.* **1997**, *79*, 4497.
(3) Emsellem, V.; Cardoso, O.; Tabeling, P. *Phys. Rev. E* **1998**, *58*, 4807.
(4) Shibuya, A.; Saito, Y.; Hyuga, H. *J. Phys. Soc. Jpn.* **2002**, *71*, 1780.
(5) D'Onofrio, T. G.; et al. *Langmuir* **2003**, *19*, 1618.
(6) Chaïeb, S.; Rica, S. *Phys. Rev. E* **1998**, *58*, 7733.
(7) Góźdź, W. T.; Gompper, G. *Europhys. Lett.* **2001**, *55*, 587.
(8) Disher, B. M.; et al. *Science* **1999**, *284*, 1143.
(9) Discher, D. E.; Eisenberg, A. *Science* **2002**, *297*, 967.
(10) Reinecke, A. A.; Döbereiner, H.-G. *Langmuir* **2003**, *19*, 605.
(11) Bar-Ziv, R.; Moses, E. *Phys. Rev. Lett.* **1994**, *73*, 1392.
(12) Bar-Ziv, R.; Moses, E.; Nelson, P. *Biophys. J.* **1998**, *75*, 294.
(13) Nelson, P.; Powers, T.; Seifert, U. *Phys. Rev. Lett.* **1995**, *74*, 3384.
(14) Tsafrir, I.; et al. *Phys. Rev. Lett.* **2001**, *86*, 1138.
(15) Tsafrir, I.; et al. *Phys. Rev. Lett.* **2003**, *91*, 138102.
(16) Helfrich, W. *Z. Naturforsch.* **1973**, *28 c*, 693.
(17) Evans, E. *Biophys. J.* **1974**, *14*, 923.
(18) Canham, P. B. *J. Theor. Biol.* **1970**, *26*, 61.
(19) Seifert, U.; Berndl, K.; Lipowsky, R. *Phys. Rev. E* **1990**, *44*, 1182.
(20) Miao, L.; Fourcade, B.; Rao, M.; Wortis, M. *Phys. Rev. A* **1991**, *43*, 6843.
(21) Heinrich, V.; Božič, B.; Svetina, S.; Žekš, B. *Biophys. J.* **1999**, *76*, 2056.
(22) Božič, B.; et al. *Eur. Biophys. J.* **2002**, *31*, 487.
(23) Brückner, E.; Sonntag, P.; Rehage, H. *Langmuir* **2001**, *17*, 2308.
(24) Góźdź, W. T. *Langmuir* **2004**, *20*, 7385.